DEP domain-containing 1 is a prognostic biomarker associated with the cell cycle in gliomas

HAIMA LI[1,2*], YEZU LIU[3*], HANWEN ZHANG[3] and XUELIAN WANG[2]

[1]Department of Neurosurgery, Shaanxi Nuclear Industry 215 Hospital, Xianyang, Shaanxi 712000, P.R. China;
[2]Department of Neurosurgery, Tangdu Hospital, Fourth Military Medical University, Xi'an, Shaanxi 710038, P.R. China;
[3]Department of Neurosurgery, Peking University People's Hospital, Beijing 100044, P.R. China

Received August 9, 2024; Accepted March 11, 2025

DOI: 10.3892/ol.2025.15022

Abstract. Glioma is the most common primary tumor in the intracranial region, accounting for more than one-half of all central nervous system tumors. Abnormal expression of key cancer genes often promotes the occurrence and development of tumors. DEP domain containing 1 (DEPDC1) is a gene that encodes a protein containing a DEP domain, which serves an important role in numerous biological processes. In the present study, the relationship between the expression level of DEPDC1 and the clinical features of glioma was explored in datasets from the China Glioma Genome Atlas Project. Kaplan-Meier survival analysis was performed to evaluate the value of DEPDC1 expression in the prognosis of patients with glioma. T-test and univariate Cox analysis were used to identify differential genes, and Gene Ontology and gene set enrichment analysis (GSEA) were used to explore the function and related mechanisms of DEPDC1 in glioma. Univariate cox and multivariate cox analyses were used to screen variables, and a nomogram model was used to construct a prediction model. In glioma U87 and LN229 cell lines, the expression of DEPDC1 was decreased using shRNA to assess the effects of DEPDC1 on the proliferation, migration and invasion of glioma cells. The findings revealed that there was a positive association between the expression level of DEPDC1 and the poor clinical features of glioma, and patients with high expression of DEPDC1 had a significantly shorter overall survival time. GSEA demonstrated that the differential genes in the DEPDC1 high expression group were mainly enriched in 'cell cycle' and 'mitotic cell cycle'. Cell experiments showed that silencing DEPDC1 in U87 and LN229 cells significantly attenuated cell proliferation, migration and invasion. To conclude, the present study demonstrates that DEPDC1 is an independent prognostic indicator for patients with glioma and is associated with a poor prognosis. The expression of DEPDC1 is closely associated with the cell cycle of glioma and provides individualized treatment options for tumors.

Correspondence to: Professor Xuelian Wang, Department of Neurosurgery, Tangdu Hospital, Fourth Military Medical University, 569 Xinsi Road, Baqiao, Xi'an, Shaanxi 710038, P.R. China
E-mail: nneurosurgery@163.com

*Contributed equally

Key words: DEP domain containing 1, glioma, bioinformatics, cell cycle, prognostic biomarkers

Introduction

Gliomas are the most common type of primary intracranial tumors in adults, accounting for ~81% of malignant brain tumors in the United States between 2014-2018 (1). According to the 2021 World Health Organization (WHO) classification of central nervous system (CNS) tumors, gliomas are divided into grades 1-4, with grades 1 and 2 classed as low-grade gliomas and grades 3 and 4 classed as high-grade gliomas (2). Currently, treatment methods for gliomas include maximal safe resection, chemoradiotherapy (3) and emerging therapies, such as immunotherapy (4) and tumor-treating field therapy (5). Treatment outcomes for gliomas are influenced by several factors, including the tumor size, location, type, pathological grade and genetic characteristics. Some gliomas are challenging to resect and may respond poorly to radiation and chemotherapy, often resulting in suboptimal treatment outcomes (6).

Gliomas account for ~81% of all malignant brain tumors and 30% of all brain and CNS tumors (7). The global incidence is estimated at 5-6 cases per 100,000 individuals annually, with glioblastoma (GBM) being the most aggressive subtype, representing 45-50% of all gliomas (2). Patients typically present with neurological symptoms such as persistent headaches, seizures, cognitive impairment and focal deficits, which vary according to tumor location and progression (8,9). High-grade gliomas, particularly GBM, are associated with a poor prognosis, with a median survival of ~15 months despite standard therapies (10). Diagnosis is primarily based on MRI, but definitive confirmation requires histopathological and molecular assessment, including isocitrate dehydrogenase (IDH) mutation status and O6-methylguanine DNA methyltransferase (MGMT) promoter methylation (11,12). Given the aggressive nature of gliomas and the challenges in treatment, ongoing research aims to identify novel biomarkers and therapeutic targets to improve patient outcomes.

As a newly discovered tumor-related gene, DEP domain containing 1 (DEPDC1) was first identified in bladder cancer by Kanehira *et al* (13) in 2007. More recently, the overexpression of DEPDC1 has been widely reported in malignant tumors originating from several organs, including the liver (14), lung (15), colon (16), breast (17), bone (18) and prostate (19). Previous research has demonstrated that DEPDC1 serves a key role in tumorigenesis by contributing to cellular functions, such as promoting cell proliferation and cell cycle progression, while suppressing apoptosis (20-22). However, few studies have investigated the role of DEPDC1 in the development and prognosis of gliomas.

In the present study, the relationship between DEPDC1 expression levels and the clinical characteristics of gliomas was explored by analyzing online databases and further examining the functional role of DEPDC1 through Gene ontology (GO) and gene set enrichment analysis (GSEA). The present study aimed to investigate the potential role of DEPDC1 in gliomas, with a focus on its association with tumor progression and patient prognosis. Understanding the implications of DEPDC1 expression could potentially contribute to the development of targeted therapeutic strategies for glioma management in the future.

Materials and methods

Data source. The present study utilized publicly available datasets from the China Glioma Genome Atlas (CGGA), including Cohort 1 (accession no. CGGA_325) and Cohort 2 (accession no. CGGA_693), to analyze the expression of DEPDC1 in gliomas. The raw Fastq data for these datasets are available under the BIGD accession numbers PRJCA001746 (Cohort 1) and PRJCA001747 (Cohort 2). Cohort 1 and 2 consist of gene expression data and clinical profiles of patients with glioma, providing valuable insights into tumor biology and disease progression. The original studies detailing these datasets can be obtained from previous CGGA publications (23,24). Glioma gene expression and clinical data were downloaded from the CGGA database (https://www.cgga.org.cn/download.jsp), which includes variables such as the sex, age, WHO grade (2), IDH mutation status, 1p/19q co-deletion status, MGMT promoter methylation status and survival information. Additionally, the Glioma Longitudinal Analysis (GLASS) dataset (http://synapse.org/glass) was used as the validation cohort. To elucidate the relationship between DEPDC1 expression and glioma prognosis, the present study analyzed its association with key clinical features using data from the CGGA database. Specifically, two RNA sequencing datasets were used, CGGA Cohort 1 and CGGA Cohort 2, comprising 325 and 693 glioma samples, respectively.

In the CGGA Cohort 1 dataset, patients were divided into a high expression level group (≥0.56) and a low expression group (<0.56), using the median DEPDC1 expression as the cut-off value. Similarly, for CGGA Cohort 2, the median DEPDC1 expression value of 0.21 was used to stratify patients into high and low expression groups. These thresholds were applied to assess the prognostic significance of DEPDC1 expression in glioma patients.

Relationship between DEPDC1 and clinical features. The association between the expression of DEPDC1 and common prognostic features was analyzed. The key features, including WHO classification (grades 1-4), IDH mutation status (wild type/mutant), primary vs. recurrent tumor status, 1p/19q deletion status (coding/non-coding deletion), age, sex, MGMT promoter methylation and DEPDC1 expression, were compared. Patients with glioma were divided into two groups based on high or low DEPDC1 expression levels, and survival curves were generated using Kaplan-Meier analysis. The Kaplan-Meier analysis was performed using overall survival (OS) as the survival metric, with time measured in months from the initial diagnosis to either the last follow-up or death.

Gene enrichment analysis. Differentially expressed genes (DEGs) between high and low DEPDC1 expression groups was identified using the 'samr' package (version 3.0; https://cran.r-project.org/web/packages/samr/) in R (log2 FC>2 and P<0.05 were the criteria for screening DEGs). GSEA (https://www.gsea-msigdb.org/gsea/index.jsp) was performed to identify signaling pathways significantly associated with the DEPDC1 expression levels. GSEA methods evaluate gene expression patterns across gene sets rather than focusing on individual genes, which can provide a more comprehensive view of enrichment pathways.

Construction of prediction model. Univariate and multivariate Cox proportional hazards regression analyses were performed to assess the relationship between variables and OS in CGGA and GLASS datasets. Variables with P<0.05 in the multivariate Cox regression analysis were selected to construct a prognostic risk model.

Build a nomogram. A nomogram was constructed in the training cohort using the 'rms' package (version 6.7-0; https://cran.r-project.org/web/packages/rms) in R. The upper portion of the nomogram represents the scoring system, whereas the lower portion represents the prediction system. Based on the scores for each factor and the total score, this tool accurately predicts the 1-, 3- and 5-year survival rates of patients with glioma. Calibration curves and C-index values were used to evaluate the accuracy of the survival predictions.

Cell lines and agents. The human glioma U87 and LN229 cell lines were obtained from the Chinese Academy of Medical Science (Beijing, China). The U87 cell line is a glioblastoma of unknown origin that has been identified as an ATCC type using short tandem repeat profiling. Cells were cultured in DMEM supplemented with 10% fetal bovine serum (FBS; Gibco; Thermo Fisher Scientific, Inc.) and 1% penicillin-streptomycin (100 U/ml penicillin and 100 μg/ml streptomycin; Gibco; Thermo Fisher Scientific, Inc.), and incubated in a humidified, CO_2-rich environment (5% CO_2) at 37˚C. The β-actin antibody (cat. no. 20536-1-AP), MMP-2 (cat. no. 10373-2-AP), MMP-9 (cat. no. 10375-2-AP) and secondary antibody (cat. nos. SA00001-1 and SA00001-2) were obtained from Proteintech Group, Inc., while the DEPDC1 antibody (cat. no. ab197246) was purchased from Abcam.

Cell transfection. The lentiviral transduction in the present study was performed using a 2nd generation lentiviral system. The 293T cell line was used as the packaging cell

line, obtained from American Type Culture Collection. For transfection, 10 μg of lentiviral plasmid, 5 μg of packaging plasmid (psPAX2) and 2.5 μg of envelope plasmid (pMD2.G) were used in a 4:2:1 ratio. Transfection was carried out at 37˚C for 6 h, after which the medium was replaced with fresh culture medium. Lentiviral particles were collected 48 h post-transfection by harvesting the supernatant and filtering it through a 0.45-μm filter. The multiplicity of infection used for infecting target cells was 10. Transduction was carried out by incubating the target cells with viral particles at 37˚C for 24 h, followed by a medium change. After 72 h, cells were subjected to subsequent experiments.

To establish stable cell lines, puromycin selection was performed using a concentration of 2 μg/ml for 7 days. Once the selection was complete, cells were maintained in 1 μg/ml puromycin for continued culture. U87 and LN229 cells were seeded at a density of $2x10^5$ cells per well in 6-well plates and the DEPDC1 gene was silenced using pLKO.1 lentiviral transduction containing DEPDC1-targeting shRNA in both cell lines. The DEPDC1-shRNA and negative control shRNA were designed by Suzhou GenePharma Co., Ltd., using the following sequences: shDEPDC1 sense, 5'-GAACTATCAAGAGTAGTT CGT-3' and antisense, 5'-UUGUUCUGAAUACAUCUCGTT-3'; and shCtrl sense, 5'-GUACCGCACGUCAUUCGUAUC-3' and antisense, 5'-UACGAAUGACGUGCGGUACGU-3'.

Reverse transcription quantitative polymerase chain reaction (RT-qPCR). Total RNA was extracted from the transfected cells using TRIzol® reagent (Invitrogen; Thermo Fisher Scientific, Inc.) according to the manufacturer's protocol. Reverse transcription was performed using the GoScript Reverse Transcription System (Promega Corporation) and RT-qPCR was performed with SYBR Premix Ex Taq II (Takara Bio, Inc.), following the manufacturers' instructions. Relative mRNA levels of DEPDC1 were normalized against GAPDH using the $2^{-\Delta\Delta Cq}$ formula (25). The primer sequences were as follows: DEPDC1 forward, 5'-TTCTAGATCTCC CTGAACCTCT-3'; and reverse, 5'-TGATGTAGCCACAAA CAACCAAA-3'; and GAPDH forward, 5'-GGAGCGAGA TCCCTCCAAAAT-3'; and reverse, 5'-GGCTGTTGTCAT ACTTCTCATGG-3'. The thermocycling conditions were as follows: 95˚C for 2 min; 40 cycles of 95˚C for 10 sec, 60˚C for 30 sec and 72˚C for 30 sec. To ensure consistency and reliability, each experiment included three technical replicates.

Western blotting. After transfection, cells were harvested for western blot analysis. Total cellular protein was extracted using RIPA buffer (Beyotime Institute of Biotechnology), quantified using a BCA assay (Beyotime Institute of Biotechnology). Subsequently, 20 μg of each protein sample was loaded per lane and separated on a 10% SDS-PAGE gel. Following electrophoresis, proteins were transferred onto PVDF membranes (Sigma-Aldrich; Merck KGaA) for further analysis. Membranes were blocked with 5% bovine serum albumin for 1 h at room temperature and incubated with the primary antibodies anti-DEPDC1 (cat. no. ab197246; 1:1,000; Abcam), anti-MMP-2 (cat. no. 10373-2-AP; 1:1,000; Proteintech Group, Inc.), anti-MMP-9 (cat. no. 10375-2-AP; 1:1,000; Proteintech Group, Inc.) and anti-β-actin (cat. no. 66009-1-Ig; 1:2,000; Proteintech Group, Inc.) overnight at 4˚C. After washing, the membranes were incubated with HRP-conjugated goat anti-rabbit IgG (cat. no. SA00001-2; Proteintech Group, Inc.) and HRP-conjugated goat anti-mouse IgG (cat. no. SA00001-1; Proteintech Group, Inc.) antibodies at a dilution of 1:5,000 at room temperature for 1.5 h, followed by three 15-min washes with TBST (Tris-buffered saline with 0.1% Tween-20; cat. no. P9416; Sigma-Aldrich). Protein expression levels were detected using Image Lab software (version 6.1; Bio-Rad Laboratories, Inc.) and visualized using the ECL Prime Western Blotting Detection Reagent (cat. no. GERPN2232; MilliporeSigma). The optical density of each strip was analyzed using ImageJ software (version 1.53t; National Institutes of Health). All the experiments were performed in triplicate.

Cell Counting Kit-8 (CCK-8) experiment. The CCK-8 assay was performed to evaluate the proliferation of U87 and LN229 cells following transfection. Briefly, $1x10^3$ normal and transfected cells were seeded into 96-well plates and cultured for 24, 48 or 72 h. Cell proliferation was assessed using a CCK-8 kit (GLPBIO Technology LLC) according to the manufacturer's protocol, and the absorbance was measured at a wavelength of 450 nm after incubation with the CCK-8 reagent for 2 h at 37˚C.

Wound healing assay. A wound healing assay was performed to evaluate the migration capacity of U87 and LN229 cells following transfection. Briefly, $1x10^6$ cells were seeded in 6-well plates and cultured for 24 h. A cross-shaped scratch was made on the monolayer of cells using a sterile 10-μl pipette tip. The scratched area was washed three times with PBS to remove the cell debris. The cells were then cultured in a serum-free medium for an additional 24 h and images of the wound area were captured. The wound area, distance between wound edges and cell confluence were measured using ImageJ software (version 1.53t; National Institutes of Health). Scratch closed rate=(initial scratch width-scratch width after 24 h)/initial scratch width x100%. The assay was repeated three times, and images were captured using an Olympus IX73 inverted fluorescence microscope (Olympus Corporation).

Transwell experiment. The invasive potential of U87 and LN229 cells after transfection was assessed using a Transwell assay. Prior to seeding, Matrigel was thawed on ice overnight at 4˚C, diluted to a final concentration of 2 mg/ml with cold serum-free medium and 50-100 μl was added to the upper chamber of each Transwell insert. The plate was incubated at 37˚C for 30-60 minto allow the Matrigel to polymerize. Serum-free cells ($1x10^5$ cells/well) were seeded in the upper chambers, whereas the lower chambers contained 10% FBS, which served as a chemoattractant. The cells were cultured at 37˚C for 12 h and subsequently washed three times with PBS. Cells on the lower surface of the membrane were fixed with 4% paraformaldehyde at room temperature for 20 min and subsequently stained with crystal violet at room temperature for 30 min. Subsequently, the stained cells were imaged using an Olympus IX73 inverted microscope (Olympus Corporation) and counted using ImageJ software (version 1.53t; National Institutes of Health). This assay was performed in triplicate.

Statistical analysis. All statistical analyses were performed using the R software (version 3.6.2; Institute for Statistical

Computing, Vienna, Austria), GraphPad Prism 9.0 (Dotmatics) or SPSS 18.0 (SPSS, Inc.). Kaplan-Meier analyses were performed using log-rank tests to assess survival differences between the groups, and the analyses were conducted using the 'survival' and 'survminer' R software packages. c^2 tests were used to evaluate the differences in clinical and molecular characteristics between the different DEPDC1 expression groups. Univariate and multivariate Cox regression analyses were performed to identify the prognostic factors. Unpaired t-tests were performed to test the significance of differences between the two groups. P<0.05 was considered to indicate a statistically significant difference.

Results

Expression of DEPDC1 and its association with clinical characteristics and prognosis of gliomas. With advancing research on gliomas, several molecular markers have been identified as pivotal for understanding the pathogenesis and diagnosis of gliomas, including IDH and 1p19q status (26,27). To elucidate the relationship between DEPDC1 expression and glioma prognosis, the association between DEPDC1 expression and key clinical features of glioma was examined in the present study using data from the CGGA Cohort 1 and 2 datasets. As shown in Fig. 1A and B, the expression of DEPDC1 was significantly elevated in older patients (≥42 years), patients with a high histological grade (CNS WHO grades 3 and 4), those with IDH wild-type gliomas, patients with 1p19q non-codel gliomas and those with recurrent tumors. Although similar trends were observed in the GLASS dataset (Fig. S1A), the association between DEPDC1 and tumor recurrence was not statistically significant. These findings suggest that expression of DEPDC1 is enriched in patients with glioma with high malignancy.

To further investigate the prognostic implications of DEPDC1 expression differences, a Kaplan-Meier survival analysis was performed. As illustrated in Fig. 1C and D, patients from both the CGGA Cohort 1 and 2 datasets were stratified into high and low DEPDC1 expression groups. The analysis revealed that patients with low DEPDC1 expression had a significantly improved prognosis compared with those patients with high DEPDC1 expression (P<0.0001). These results were validated using a GLASS cohort (Fig. S1B) (P<0.0001), with outcomes consistent with those observed in CGGA cohort 325 (Cohort 1) and CGGA cohort 693 (Cohort 2). Collectively, these findings indicate that high expression of DEPDC1 is associated with shorter survival times, suggesting it has potential as a prognostic marker in gliomas.

GO analysis of DEGs and GSEA enrichment analysis. To further investigate the potential mechanisms by which DEPDC1 contributes to the deterioration of prognosis in patients with glioma, the pathways that DEPDC1 modulates were examined. Patients were divided into two groups based on the median expression of DEPDC1, with the low expression group serving as the control. In CGGA Cohort 1, 957 genes were upregulated (log2 FC >2; P<0.05). GO analysis was performed on the DEGs. GO analysis revealed the top enriched pathways associated with DEPDC1 expression, with the top five pathways including 'cell cycle', 'mitotic cell cycle', 'extracellular matrix organization', 'vasculature development' and 'NABA core matrisome' (Fig. 2A). In CGGA Cohort 2, 324 genes were upregulated in the high expression group (Log2 FC >2; P<0.05). GO analysis identified DEPDC1-related pathways among the significantly enriched terms, with the top five being 'mitotic cell cycle', 'tube morphogenesis', 'embryonic morphogenesis', 'regulation of cell cycle process' and 'extracellular matrix organization' (Fig. 2C). These findings were consistent with the data shown in Fig. 2A. While 'inflammatory response' and 'cytokine signaling in the immune system' were not the highest-ranked pathways by statistical significance, they were highlighted due to their potential involvement in the glioma microenvironment and immune regulation. Therefore, both datasets predominantly showed enrichment in the cell cycle, vascular development and immune-related pathways. GSEA was performed to confirm these findings. As shown in Fig. 2B and D, the main enriched pathways identified using GSEA included 'cell cycle', 'DNA replication', 'spliceosome' and 'nucleotide excision repair'. These results confirmed that DEPDC1 is closely associated with the glioma cell cycle, immune response and vascular development. Similar results were obtained for the GLASS dataset (Fig. S2).

Expression of DEPDC1 is closely associated with the cell cycle. To further explore the mechanism through which DEPDC1 regulates glioma cell proliferation, its relationship with established cell cycle checkpoints was examined. The analysis revealed that checkpoint kinase 1 (CHEK1), cyclin-dependent kinase 7 (CDK7) and tumor protein 53 (TP53) were positively associated with the expression of DEPDC1 in both CGGA Cohorts 1 and 2 (Fig. 3A and B). A similar trend was observed in the GLASS cohort (Fig. S3B), although the correlation between DEPDC1 and CDK7 appears less pronounced compared with other cell cycle-related genes. These results indicate that the expression of DEPDC1 may serve a role in the regulation of glioma cell cycle progression.

DEPDC1 is an independent prognostic factor in patients with glioma. To further evaluate the role of DEPDC1 in the prognosis of patients with glioma, receiver operating characteristic analysis was used to assess the ability of DEPDC1 expression to predict patient outcomes. As shown in Fig. 4A, in CGGA Cohort 1, the area under the curve (AUC) was 0.78 at 1 year, 0.85 at 3 years and 0.85 at 5 years. As shown in Fig. 4B, in CGGA Cohort 2, the AUC reached 0.67 at 1 year, 0.76 at 3 years and 0.79 at 5 years, respectively. Similarly, in the GLASS dataset (Fig. S3A), the AUC values were 0.61 at 1 year, 0.75 at 3 years, and 0.85 at 5 years. In CGGA Cohort 1 (CGGA_325), the AUC values were 0.78 at 1 year, 0.85 at 3 years and 0.85 at 5 years (Fig. 4A), while in the CGGA Cohort 2, the AUC values were 0.67 at 1 year, 0.76 at 3 years and 0.79 at 5 years (Fig. 4B). Univariate and multivariate Cox regression analyses of CGGA Cohorts 1 and 2 indicated that DEPDC1 is an independent prognostic factor for patients with glioma (Fig. 4C-F). Similar results were observed for the GLASS dataset (Fig. S3C and D). These results suggested that expression of DEPDC1 is an independent prognostic factor for OS.

Individualized prediction model shows high accuracy. Independent prognostic indicators of OS were selected and

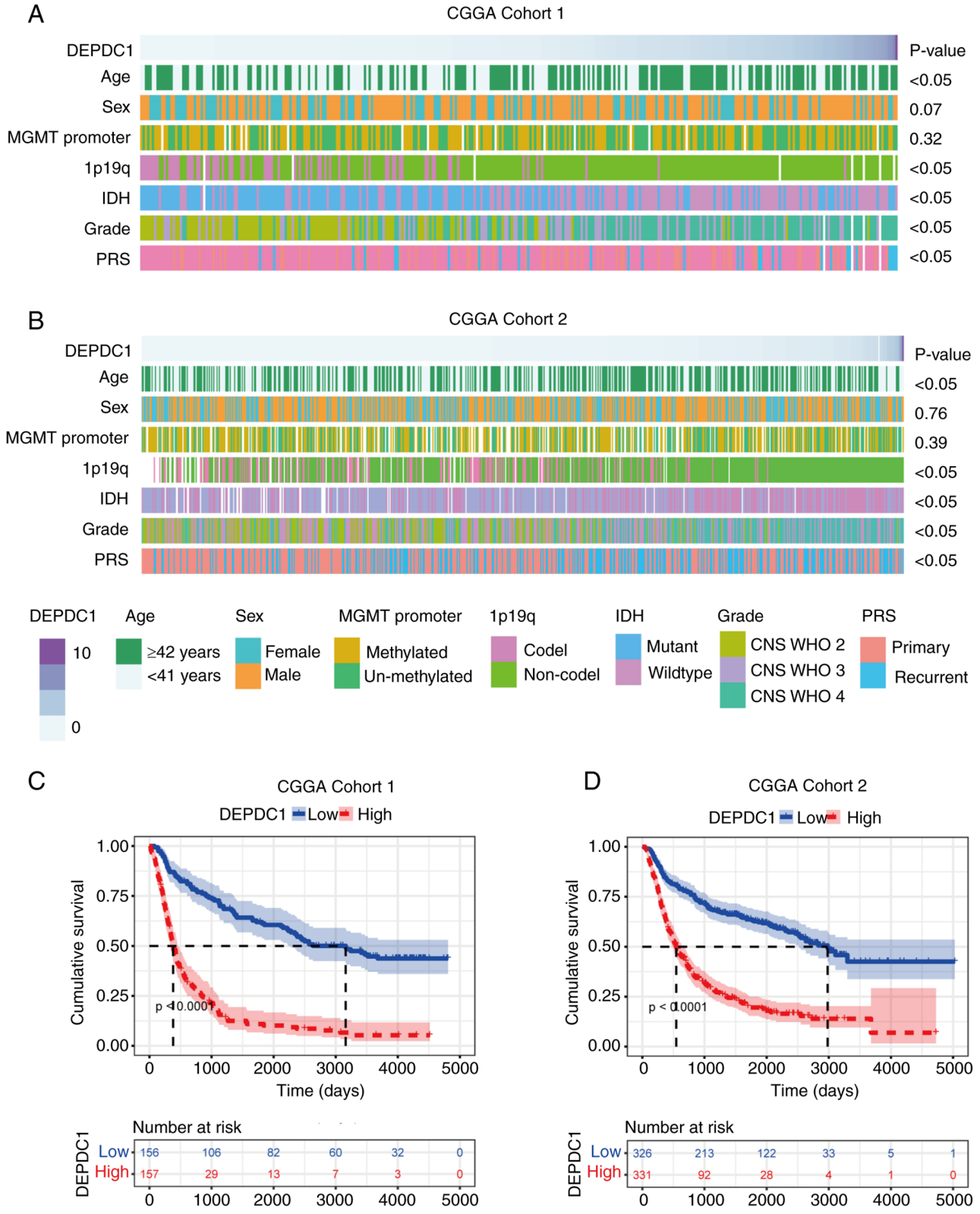

Figure 1. Relationship between DEPDC1, clinicopathological features and prognosis of glioma. (A) Association between DEPDC1 expression and clinicopathological features of patients with glioma in the CGGA Project Cohort 1 database. (B) Association between DEPDC1 and clinicopathological features of gliomas in the CGGA Cohort 2 database. Kaplan-Meier analysis illustrating the prognostic significance of DEPDC1 expression in (C) CGGA Cohort 1 and (D) CGGA Cohort 2. DEPDC1, DEP domain containing 1; CGGA, China Glioma Genome Atlas; IDH, isocitrate dehydrogenase; CNS, central nervous system; WHO, World Health Organization; PRS, polygenic risk score.

integrated into multivariate regression analysis to construct a prediction model. In the CGGA Cohort 1 dataset, patients were divided into a high expression group (≥0.56) and low expression group (<0.56), with the median DEPDC1 expression as the cut-off value. High and low expression of DEPDC1 contributed to risk scores from 0 to 100 (Fig. 5A).

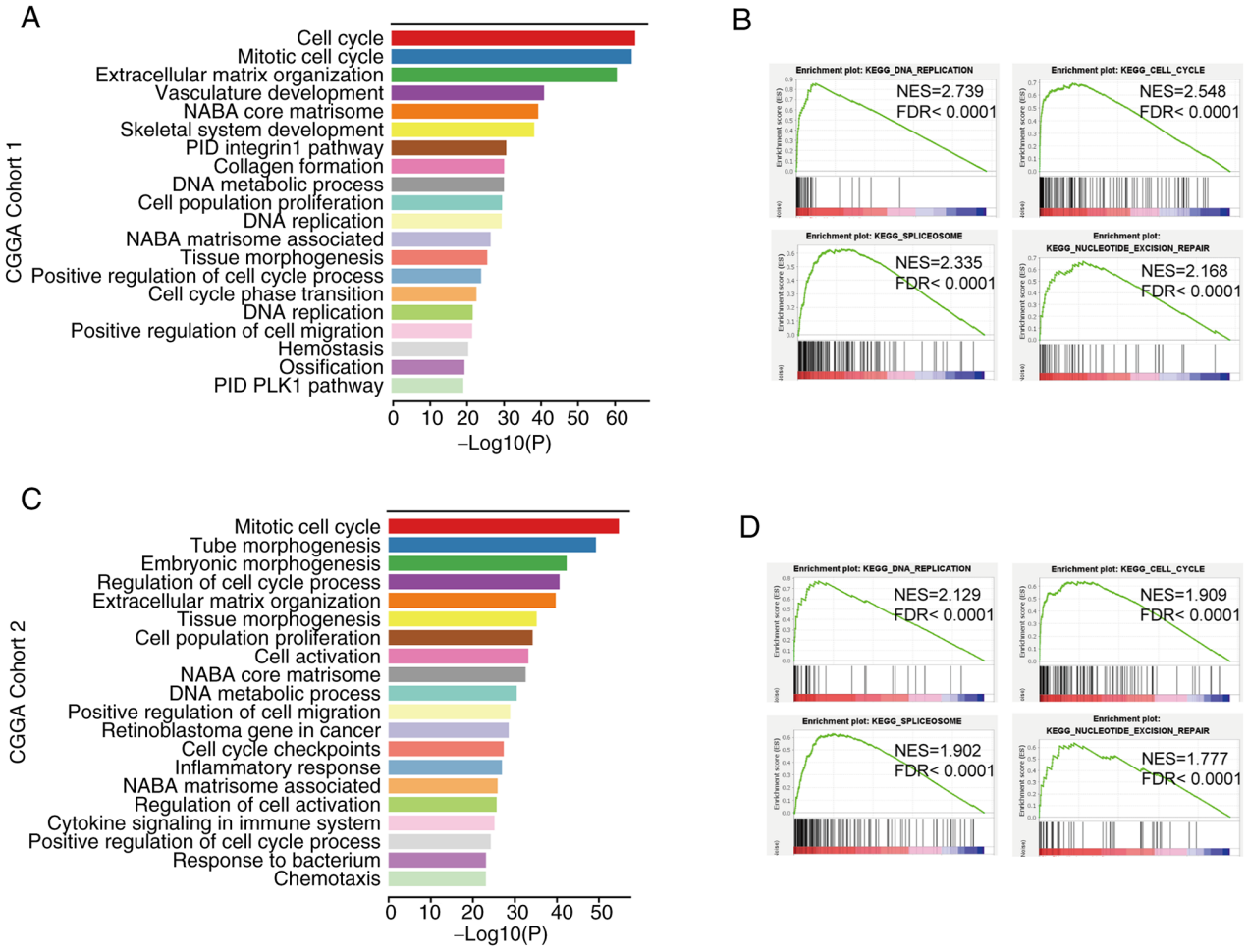

Figure 2. GO analysis and GSEA of DEGs associated with DEPDC1 expression. (A) Upregulated DEGs were analyzed using GO in CGGA database Cohort 1. (B) The top enrichment pathways were identified using GSEA in Cohort 1. (C) GO analysis and (D) GSEA were performed in CGGA database Cohort 2. GO, Gene Ontology; GSEA, gene set enrichment analysis; DEPDC1, DEP domain containing 1; CGGA, China Glioma Genome Atlas; FDR, false discovery rate; NES, normalized enrichment score.

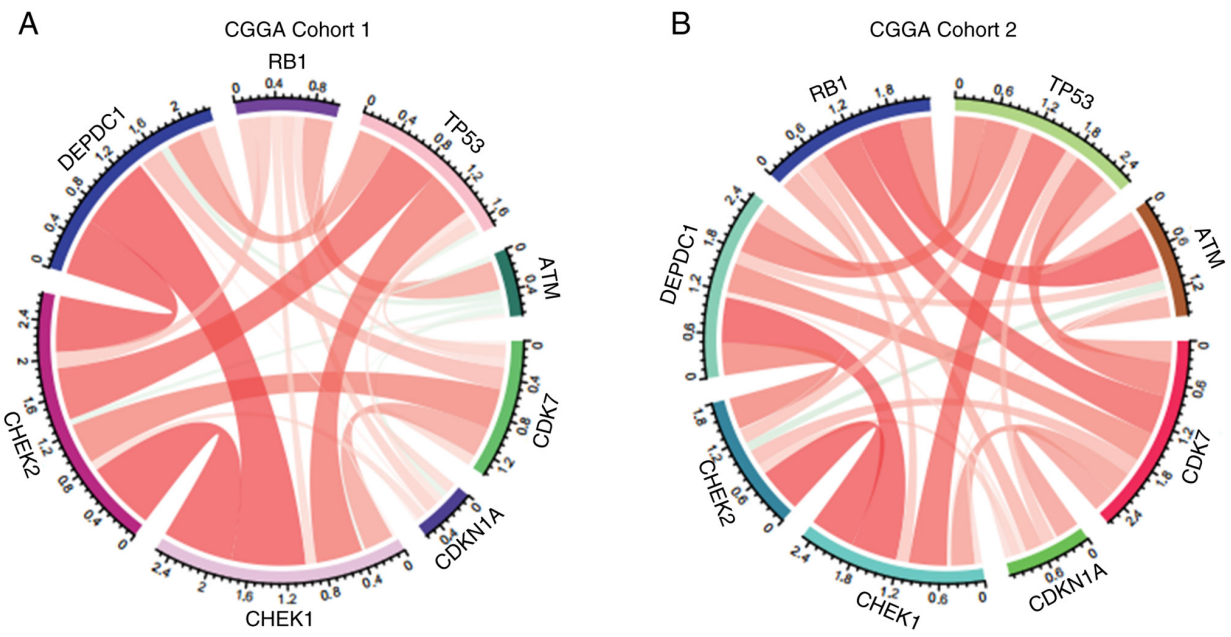

Figure 3. DEPDC1 is closely associated with the regulation of cell cycle processes. Association analysis of DEPDC1 expression and cell cycle checkpoints in CGGA (A) Cohort 1 and (B) Cohort 2 datasets. DEPDC1, DEP domain containing 1; CGGA, China Glioma Genome Atlas; RB1, RB transcriptional corepressor 1; TP53, tumor protein 53; ATM, ATM serine/threonine kinase; CDK7, cyclin-dependent kinase 7; CDKN1A, cyclin-dependent kinase inhibitor 1A; CHEK, checkpoint kinase.

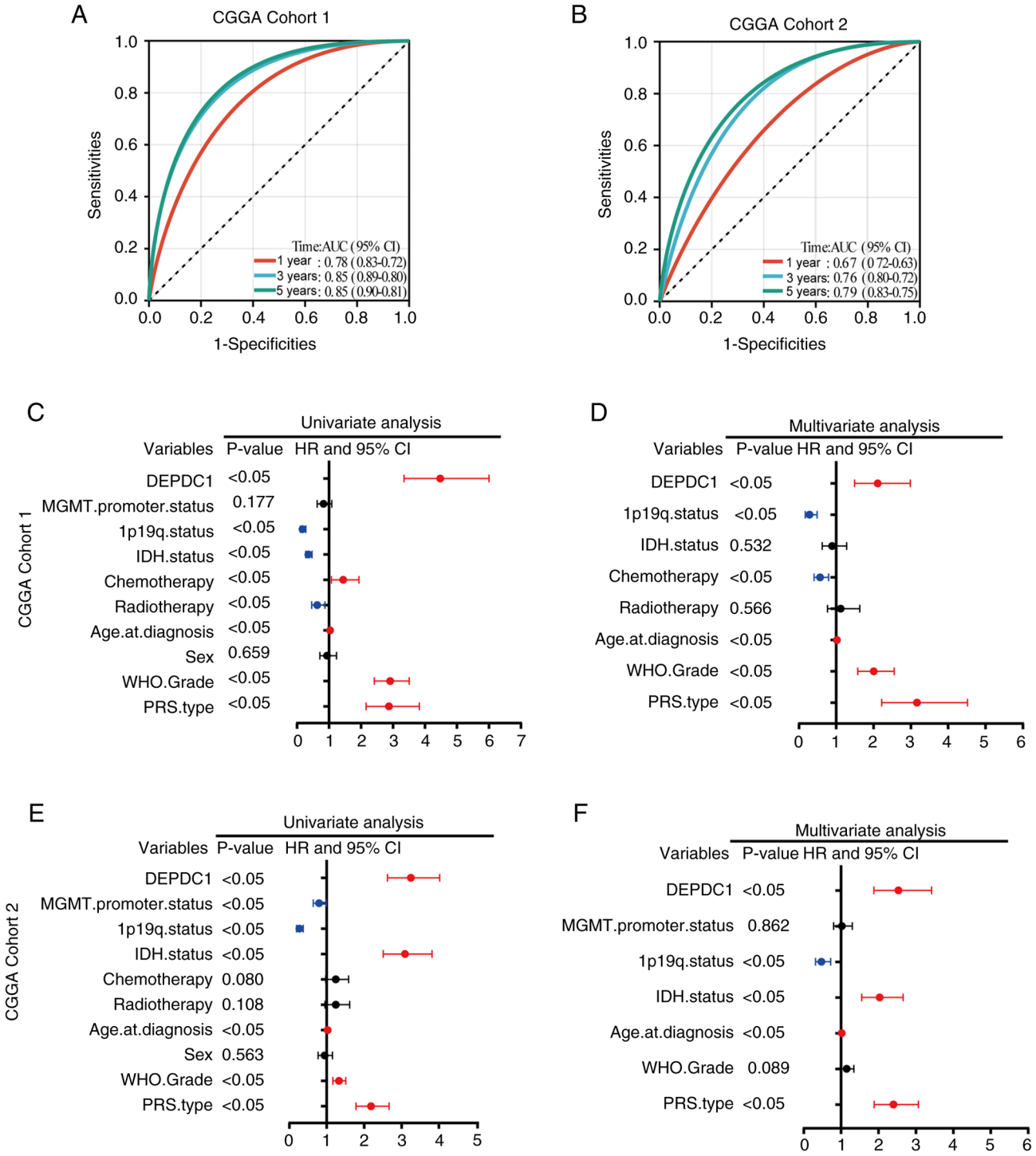

Figure 4. DEPDC1 is associated with the prognosis of patients with glioma. Time-dependent ROC analysis results predicting OS of patients at 1 (red), 3 (blue) and 5 (green) years based on DEPDC1 expression in CGGA (A) Cohort 1 and (B) Cohort 2. Forest plots show (C) univariate and (D) multivariate Cox regression analyses of DEPDC1 and clinicopathological features in CGGA Cohort 1. Forest plots show (E) univariate and (F) multivariate Cox regression analysis in CGGA Cohort 2. DEPDC1, DEP domain containing 1; CGGA, China Glioma Genome Atlas; HR, hazard ratio; CI, confidence interval; IDH, isocitrate dehydrogenase; AUC, area under the curve; PRS, polygenic risk score.

In CGGA Cohort 1, the C-index of the nomogram was 0.810. The calibration plot demonstrated a good agreement between the predicted and observed 1-, 3- and 5-year OS probabilities (Fig. 5B). Similar results were validated in the CGGA Cohort 2 (Fig. 6) and GLASS datasets (Fig. S4), with C-indices of 0.771 and 0.763, respectively, indicating the high accuracy of the DEPDC1 score.

Expression of DEPDC1 is associated with the proliferation and invasion of gliomas. To investigate the expression levels of DEPDC1 in U87 and LN229 cells, shRNA was used to interfere with DEPDC1 expression in both cell lines. As shown in Fig. 7A, RT-qPCR analysis indicated that DEPDC1 mRNA levels decreased significantly after silencing with shDEPDC1 compared with the control shRNA. Correspondingly, western

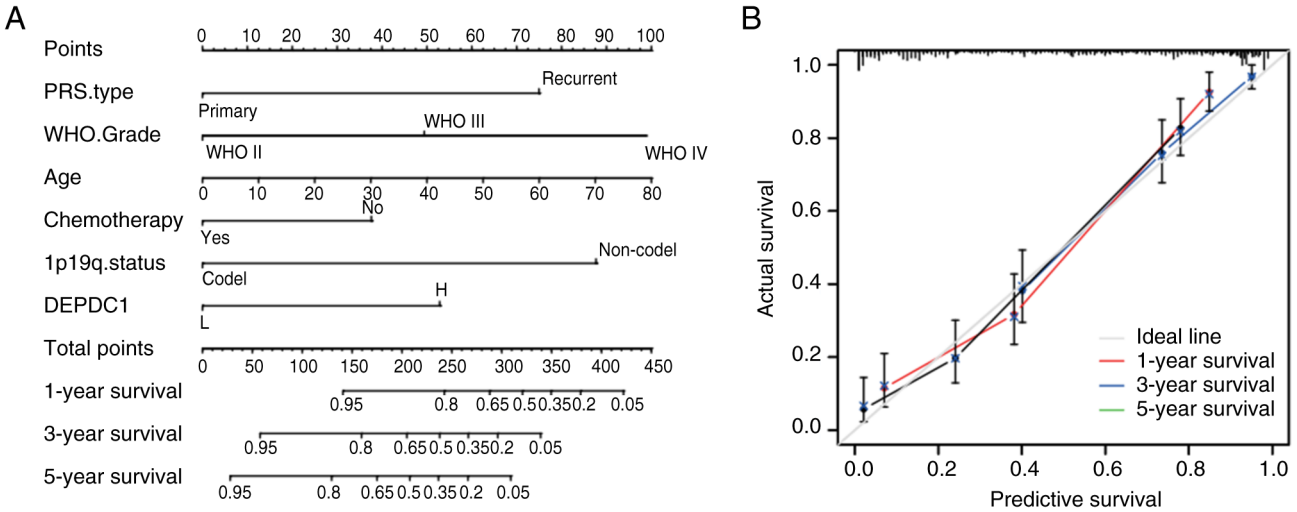

Figure 5. Construction of a personalized prediction model in the CGGA Cohort 1 dataset. (A) Nomogram constructed based on CGGA Cohort 1. (B) Calibration plot of the prognostic model showing the predicted OS for 1-, 3- and 5-year survival probabilities in CGGA Cohort 1 compared with actual OS. OS, overall survival; CGGA, China Glioma Genome Atlas; DEPDC1, DEP domain containing 1; WHO, World Health Organization; PRS, polygenic risk score.

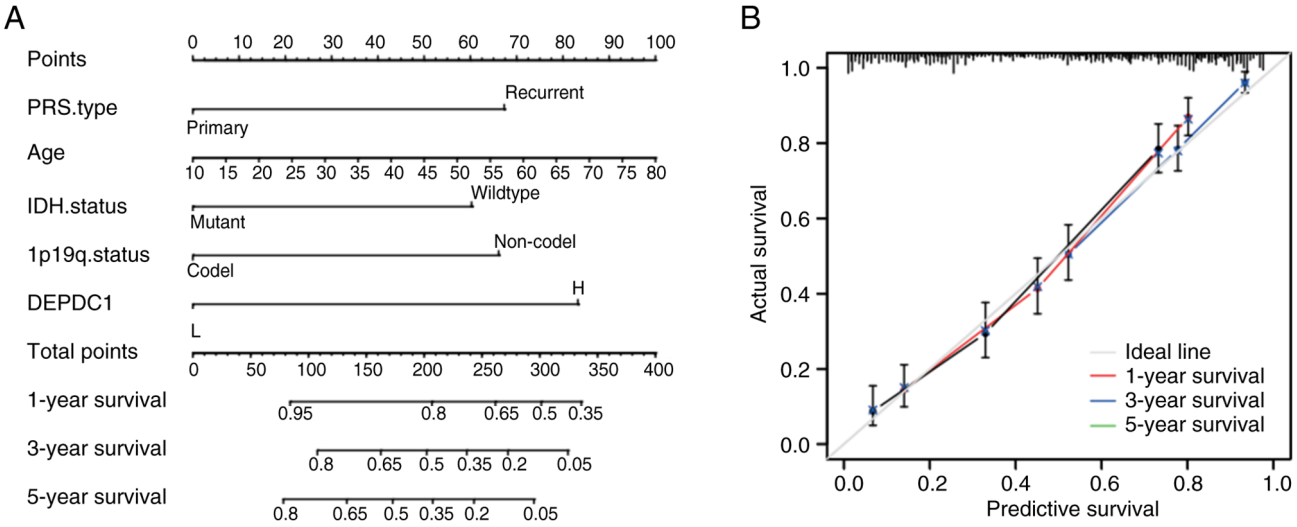

Figure 6. Construction of a personalized prediction model in the CGGA Cohort 2 dataset. (A) Nomogram constructed based on CGGA Cohort 2. (B) Calibration plot of the prognostic model showing the predicted OS for 1-, 3- and 5-year survival probabilities in CGGA Cohort 2 compared with actual OS. OS, overall survival; CGGA, China Glioma Genome Atlas; DEPDC1, DEP domain containing 1; WHO, World Health Organization; PRS, polygenic risk score.

blot analysis demonstrated that the protein expression levels also showed qualitative and semi-quantitative reductions, as shown in Fig. 7B and C. To further examine the impact of DEPDC1 expression on glioma cell proliferation and invasion, CCK-8, wound healing and Transwell invasion assays were performed. As shown in Fig. 8A, the proliferation rate of glioma cells was significantly reduced over the first 5 days following DEPDC1 silencing compared with the control shRNA. In addition, Fig. 8B shows wound healing assay results for U87 and LN229 cells, comparing cell migration over a 24 h period. At 0 h, the wound areas were similar in all groups. After 24 h, the shCtrl cells migrated more compared with the shDEPDC1 cells, indicating that DEPDC1 knockdown reduced migration. Furthermore, Fig. 8C shows the invasion assay results for U87 and LN229 cells. At 0 h, the number of invading cells was similar between groups. After 24 h, fewer cells had invaded in the shDEPDC1 group compared with the shCtrl group, indicating that DEPDC1 knockdown reduces invasion. Additionally, migration-related proteins MMP-2 and MMP-9 were markedly decreased after DEPDC1 silencing, as shown in Fig 8D. Fig. 8E demonstrates that the invasive ability of glioma cells in both cell lines was significantly impaired by DEPDC1 silencing compared with the control shRNA, as observed in the Transwell assay.

Discussion

Previous studies have indicated that DEPDC1 upregulation is closely associated with a poor prognosis in several malignant tumors, including hepatocellular carcinoma (28-31), lung adenocarcinoma (15,32), colorectal cancer (33,34), breast cancer (35) and osteosarcoma (36). A notable study further demonstrated

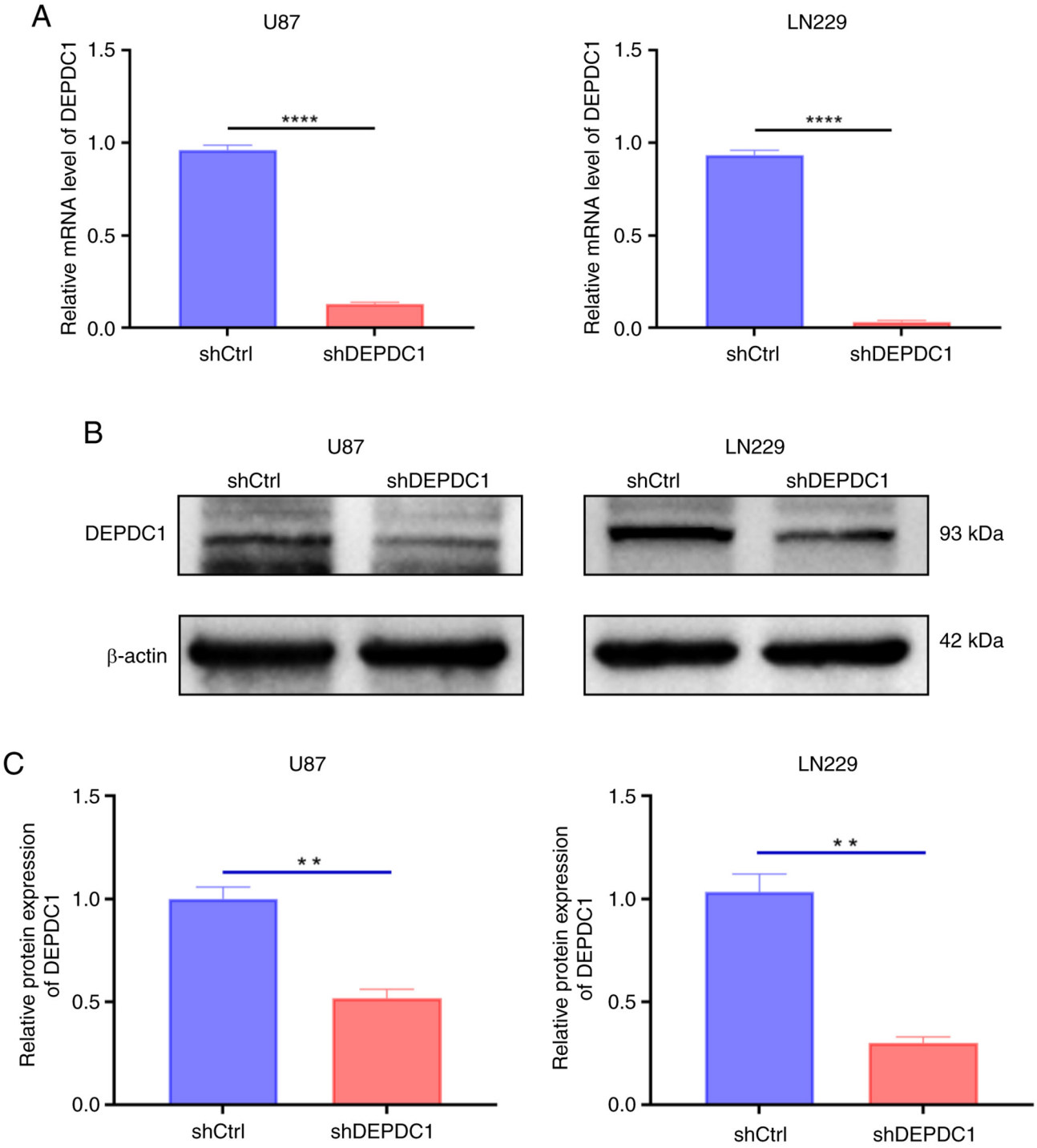

Figure 7. DEPDC1 mRNA and protein expression. (A) Relative DEPDC1 mRNA levels in shDEPDC1-treated glioma cells, in U87 and LN229 cell lines. (B) Western blotting showing relative protein expression in DEPDC1-silenced U87 and LN229 cells compared with non-silenced controls. (C) Semi-quantitative analysis of DEPDC1 protein expression in silenced glioma cells in U87 and LN229 cell lines. n=3 biological replicates. **P<0.01; ****P<0.0001 vs. shCtrl. DEPDC1, DEP domain containing 1; sh, short hairpin; Ctrl, control.

that DEPDC1 is markedly upregulated in 29 out of 33 human cancer types and is associated with OS, disease-specific survival and progression-free survival in multiple tumor types (37). In the present study, expression levels of DEPDC1 were assessed in gliomas with several typical prognostic characteristics by performing association analysis based on data from patients with glioma from the CGGA and GLASS databases. The results demonstrated that DEPDC1 is highly expressed in more aggressive gliomas, particularly in patients of older age (≥42 years), those with high histological grades (CNS WHO 3,4), those with IDH wild-type gliomas, patients with 1p/19q codeletion and cases with tumor recurrence. Kaplan-Meier analysis was performed to examine the relationship between the expression of DEPDC1 and patient prognosis, further confirming that high DEPDC1 expression significantly affects survival time. Furthermore, DEPDC1 expression was observed in human glioma U87 and LN229 cell lines. Additionally, DEPDC1 knockdown inhibited the proliferation, migration

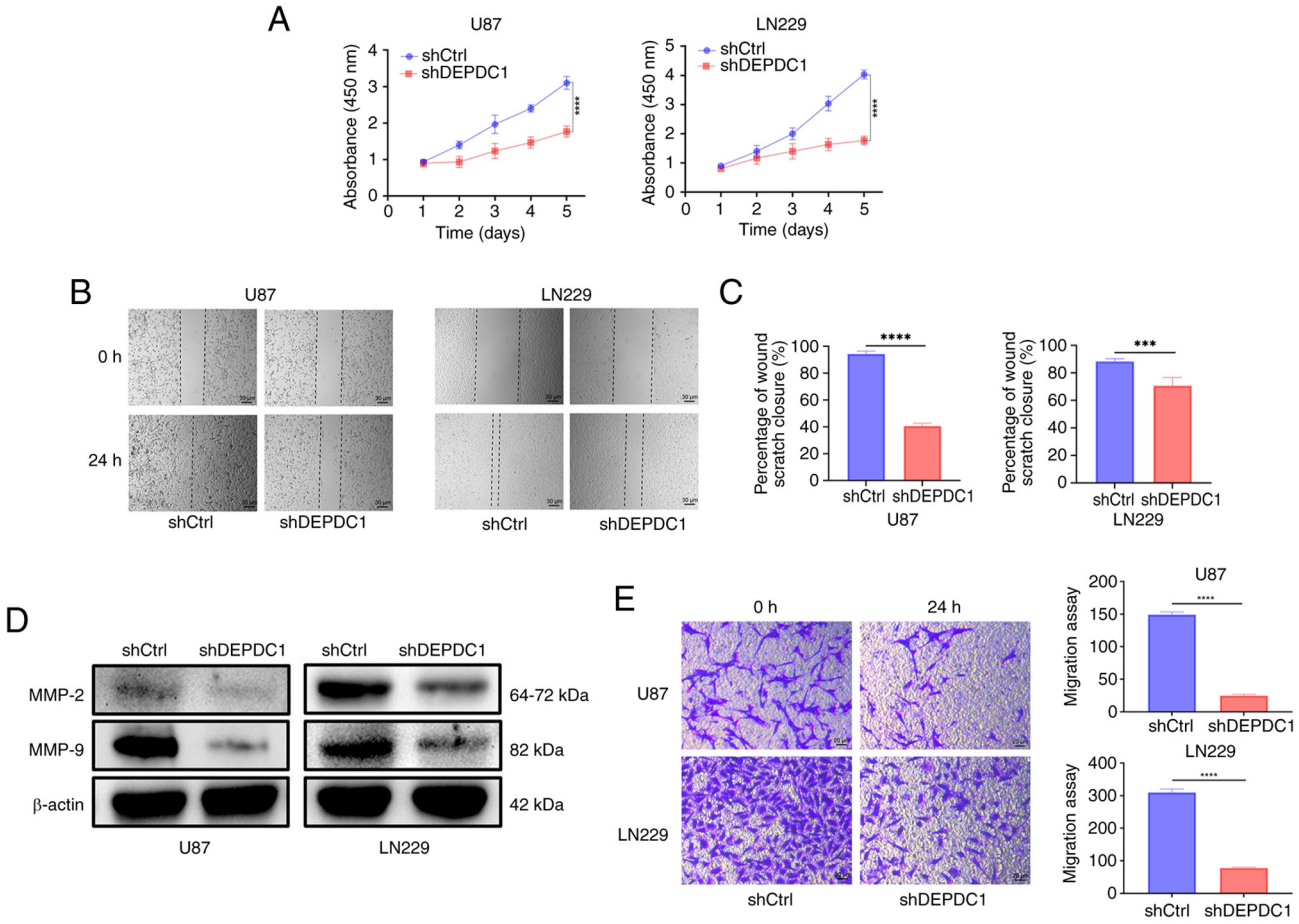

Figure 8. DEPDC1 impact on glioma cell proliferation and invasion. (A) Absorbance data plots depicting 5-day proliferation of DEPDC1-silenced glioma cells in U87 and LN229 lines compared with the control. (B) Cell migration comparison of DEPDC1-silenced vs. non-silenced U87 and LN229 cells after 24 h. (C) Quantification of scratch close rate. (D) Western blot showing a marked decreased of migration-associated proteins MMP-2 and MMP-9 in DEPDC1-silenced U87 and LN229 cell lines compared with non-silenced controls. (E) Imaging and quantitative analysis of 24-h invasion activity of DEPDC1-silenced U87 and LN229 cells in the Transwell assay. n=3 biological replicates. ***P<0.001 and ****P<0.0001 vs. shCtrl. DEPDC1, DEP domain containing 1; sh, short hairpin; Ctrl, control.

and invasion of glioma cells. This suggested that DEPDC1 serves a role in promoting glioma progression. The reduced cell motility and invasion observed after DEPDC1 knockdown were consistent with previous studies on DEPDC1-related tumor genes (17,38,39). These findings indicate that DEPDC1 may contribute to glioma malignancy and could be a potential target for further investigation.

To further investigate the potential mechanisms by which DEPDC1 contributes to glioma progression, its relationship with cell cycle regulation, immune response and vascular development was examined through GO and GSEA enrichment analyses of DEGs from two CGGA database cohorts, with results corroborated in the GLASS dataset. The findings suggest that DEPDC1 influences glioma cell proliferation and apoptosis through the expression of several specific RNAs or proteins, such as cyclin dependent kinase 1, CHEK1 and RB transcriptional corepressor 1, were affected by DEPDC1 knockdown. These findings suggest that DEPDC1 may regulate glioma progression through pathways involving cell cycle control and DNA damage response (40). Additionally, DEPDC1 may induce generation of specific T lymphocytes, potentially affecting immune system function (41) and promoting the overexpression of angiogenic factors, leading to increased glioma proliferation and blood vessel density (42).

In view of the relationship between DEPDC1 expression and the cell cycle, its association with several recognized cell cycle checkpoints was investigated. The results demonstrate expression of DEPDC1 was positively associated with CHEK1, CDK7 and TP53 expression. CHEK1 is a key signal transduction factor in the genome integrity checkpoint, and its mutations have been implicated in various cancer types, including colon, stomach and endometrial carcinomas (43). Similarly, abnormal CDK7 expression or function (44) and TP53 mutations (45) are associated with the occurrence and progression of multiple cancer types, including breast, colorectal, ovarian, head and neck and lung cancers. Thus, DEPDC1 may influence glioma progression by modulating the expression of these genes, contributing to cell cycle regulation and affecting tumor proliferation, malignancy and potential prognosis. As demonstrated in previous studies, DEPDC1 serves an important role in regulating the cell cycle and tumor progression across different cancer types via various signaling pathways. For instance, Huang *et al* (19) showed that in prostate cancer, DEPDC1 enhances E2F1 transcriptional activity, thereby upregulating cyclin D1 and CDK2, leading to a more frequent G_1-S phase cell cycle transition. Similarly, Wang *et al* (16) reported that DEPDC1 promotes SUZ12 polycomb repressive complex 2 subunit expression to drive proliferation, invasion

and epithelial-mesenchymal transition of colorectal cancer. These findings suggest a potential mechanism through which DEPDC1 regulates cell cycle progression. However, further investigations are needed to elucidate the specific mechanism of action of DEPDC1 in glioma cell cycle regulation.

In the present study, univariate and multivariate Cox regression analyses were performed and demonstrated that DEPDC1 serves as an independent prognostic factor in patients with glioma. To evaluate the accuracy of DEPDC1 as a prognostic marker, a prediction model was constructed based on 1-, 3- and 5-year survival rates using a nomogram calibrated against the CGGA database observations. These results indicate that high DEPDC1 expression adversely affects patient prognosis. If this prediction model is highly accurate, it may support clinical decision making, potentially improving patient outcomes.

The present study has certain limitations. The results demonstrated that DEPDC1 is closely associated with key genes in multiple cell cycle signaling pathways. However, the molecular interaction mechanisms have not been further elucidated in animal experiments and patient-derived glioma samples. Additionally, as patients with high-grade glioma generally have a worse prognosis, the functional role of DEPDC1 was only evaluated in two high-grade glioma cell lines. Therefore, the functions of DEPDC1 observed in the present study may not apply to low-grade gliomas. These limitations should be addressed in animal models and glioma cell lines of various grades.

In summary, the expression of DEPDC1 is closely associated with glioma cell cycle regulation and serves as an independent prognostic indicator, with higher expression levels linked to worse outcomes. DEPDC1 knockdown reduces glioma cell proliferation and migration, suggesting it has potential as a target for individualized tumor treatment.

Acknowledgements

Not applicable.

Funding

No funding was received.

Availability of data and materials

The data generated in the present study may be requested from the corresponding author.

Authors' contributions

HL and YL contributed to conceptualization, formal analysis, investigation, data curation and writing of the original draft. HZ contributed to methodology, formal analysis and reviewing of the original draft. HZ, HL and YL confirm the authenticity of all the raw data. XW contributed to conceptualization, reviewing the draft, supervision, project administration and funding acquisition. All authors read and approved the final version of the manuscript, and agree to be accountable for all aspects of the work.

Ethics approval and consent to participate

Not applicable.

Patient consent for publication

Not applicable.

Competing interests

The authors declare that they have no competing interests.

References

1. Ostrom QT, Cioffi G, Waite K, Kruchko C and Barnholtz-Sloan JS: CBTRUS statistical report: Primary brain and other central nervous system tumors diagnosed in the United States in 2014-2018. Neuro Oncol 23: iii1-iii105, 2021.
2. Louis DN, Perry A, Wesseling P, Brat DJ, Cree IA, Figarella-Branger D, Hawkins C, Ng HK, Pfister SM, Reifenberger G, *et al*: The 2021 WHO classification of tumors of the central nervous system: A summary. Neuro Oncol 23: 1231-1251, 2021.
3. Nicholson JG and Fine HA: Diffuse glioma heterogeneity and its therapeutic implications. Cancer Discov 11: 575-590, 2021.
4. Zeng J, Li X, Sander M, Zhang H, Yan G and Lin Y: Oncolytic Viro-Immunotherapy: An emerging option in the treatment of gliomas. Front Immunol 12: 721830, 2021.
5. Stupp R, Taillibert S, Kanner A, Read W, Steinberg D, Lhermitte B, Toms S, Idbaih A, Ahluwalia MS, Fink K, *et al*: Effect of tumor-treating fields plus maintenance temozolomide vs maintenance temozolomide alone on survival in patients with glioblastoma: A randomized clinical trial. JAMA 318: 2306-2316, 2017.
6. Brown CE, Hibbard JC, Alizadeh D, Blanchard MS, Natri HM, Wang D, Ostberg JR, Aguilar B, Wagner JR, Paul JA, *et al*: Locoregional delivery of IL-13Rα2-targeting CAR-T cells in recurrent high-grade glioma: A phase 1 trial. Nat Med 30: 1001-1012, 2024.
7. Ostrom QT, Cioffi G, Waite K, Kruchko C and Barnholtz-Sloan JS: CBTRUS statistical report: Primary brain and other central nervous system tumors diagnosed in the United States in 2014-2018. Neuro Oncol 23: iii1-iii105, 2021.
8. Rees JH: Diagnosis and treatment in neuro-oncology: An oncological perspective. Br J Radiol 84 Spec No 2: S82-S89, 2011.
9. Huse JT and Holland EC: Targeting brain cancer: Advances in the molecular pathology of malignant glioma and medulloblastoma. Nat Rev Cancer 10: 319-331, 2010.
10. Stupp R, Mason WP, van den Bent MJ, Weller M, Fisher B, Taphoorn MJ, Belanger K, Brandes AA, Marosi C, Bogdahn U, *et al*: Radiotherapy plus concomitant and adjuvant temozolomide for glioblastoma. N Engl J Med 352: 987-996, 2005.
11. Weller M, Stupp R, Reifenberger G, Brandes AA, van den Bent MJ, Wick W and Hegi ME: MGMT promoter methylation in malignant gliomas: Ready for personalized medicine? Nat Rev Neurol 6: 39-51, 2010.
12. Ellingson BM, Wen PY and Cloughesy TF: Modified criteria for radiographic response assessment in glioblastoma clinical trials. Neurotherapeutics 14: 307-320, 2017.
13. Kanehira M, Harada Y, Takata R, Shuin T, Miki T, Fujioka T, Nakamura Y and Katagiri T: Involvement of upregulation of DEPDC1 (DEP domain containing 1) in bladder carcinogenesis. Oncogene 26: 6448-6455, 2007.
14. Li Y, Tian Y, Zhong W, Wang N, Wang Y, Zhang Y, Zhang Z, Li J, Ma F, Zhao Z and Peng Y: Artemisia argyi essential oil inhibits hepatocellular carcinoma metastasis via suppression of DEPDC1 dependent Wnt/β-catenin signaling pathway. Front Cell Dev Biol 9: 664791, 2021.
15. Wang W, Li A, Han X, Wang Q, Guo J, Wu Y, Wang C and Huang G: DEPDC1 up-regulates RAS expression to inhibit autophagy in lung adenocarcinoma cells. J Cell Mol Med 24: 13303-13313, 2020.
16. Wang Q, Jiang S, Liu J, Ma G, Zheng J and Zhang Y: DEP domain containing 1 promotes proliferation, invasion, and epithelial-mesenchymal transition in colorectal cancer by enhancing expression of suppressor of zest 12. Cancer Biother Radiopharm 36: 36-44, 2021.
17. Zhang L, Du Y, Xu S, Jiang Y, Yuan C, Zhou L, Ma X, Bai Y, Lu J and Ma J: DEPDC1, negatively regulated by miR-26b, facilitates cell proliferation via the up-regulation of FOXM1 expression in TNBC. Cancer Lett 442: 242-251, 2019.

18. Shen L, Li H, Liu R, Zhou C, Bretches M, Gong X, Lu L, Zhang Y, Zhao K, Ning B, *et al*: DEPDC1 as a crucial factor in the progression of human osteosarcoma. Cancer Med 12: 5798-5808, 2023.
19. Huang L, Chen K, Cai ZP, Chen FC, Shen HY, Zhao WH, Yang SJ, Chen XB, Tang GX and Lin X: DEPDC1 promotes cell proliferation and tumor growth via activation of E2F signaling in prostate cancer. Biochem Biophys Res Commun 490: 707-712, 2017.
20. Yang Y, Jiang Y, Jiang M, Zhang J, Yang B, She Y, Wang W, Deng Y and Ye Y: Protocadherin 10 inhibits cell proliferation and induces apoptosis via regulation of DEP domain containing 1 in endometrial endometrioid carcinoma. Exp Mol Pathol 100: 344-352, 2016.
21. Mi Y, Zhang C, Bu Y, Zhang Y, He L, Li H, Zhu H, Li Y, Lei Y and Zhu J: DEPDC1 is a novel cell cycle related gene that regulates mitotic progression. BMB Rep 48: 413-418, 2015.
22. Sendoel A, Maida S, Zheng X, Teo Y, Stergiou L, Rossi CA, Subasic D, Pinto SM, Kinchen JM, Shi M, *et al*: DEPDC1/LET-99 participates in an evolutionarily conserved pathway for anti-tubulin drug-induced apoptosis. Nat Cell Biol 16: 812-820, 2014.
23. Zhao Z, Zhang KN, Wang Q, Li G, Zeng F, Zhang Y, Wu F, Chai R, Wang Z, Zhang C, *et al*: Chinese glioma genome atlas (CGGA): A comprehensive resource with functional genomic data from chinese glioma patients. Genomics Proteomics Bioinformatics 19: 1-12, 2021.
24. Zhang K, Liu X, Li G, Chang X, Li S, Chen J, Zhao Z, Wang J, Jiang T and Chai R: Clinical management and survival outcomes of patients with different molecular subtypes of diffuse gliomas in China (2011-2017): A multicenter retrospective study from CGGA. Cancer Biol Med 19: 1460-1476, 2022.
25. Livak KJ and Schmittgen TD: Analysis of relative gene expression data using real-time quantitative PCR and the 2(-Delta Delta C(T)) method. Methods 25: 402-408, 2001.
26. Chakrabarty S, LaMontagne P, Shimony J, Marcus DS and Sotiras A: MRI-based classification of IDH mutation and 1p/19q codeletion status of gliomas using a 2.5D hybrid multi-task convolutional neural network. Neurooncol Adv 5: vdad023, 2023.
27. Wesseling P, van den Bent M and Perry A: Oligodendroglioma: Pathology, molecular mechanisms and markers. Acta Neuropathol 129: 809-827, 2015.
28. Amisaki M, Yagyu T, Uchinaka EI, Morimoto M, Hanaki T, Watanabe J, Tokuyasu N, Sakamoto T, Honjo S and Fujiwara Y: Prognostic value of DEPDC1 expression in tumor and non-tumor tissue of patients with hepatocellular carcinoma. Anticancer Res 39: 4423-4430, 2019.
29. Yuan SG, Liao WJ, Yang JJ, Huang GJ and Huang ZQ: DEP domain containing 1 is a novel diagnostic marker and prognostic predictor for hepatocellular carcinoma. Asian Pac J Cancer Prev 15: 10917-10922, 2014.
30. Bin X, Luo Z, Wang J and Zhou S: Identification of a five immune term signature for prognosis and therapy options (Immunotherapy versus Targeted Therapy) for patients with hepatocellular carcinoma. Comput Math Methods Med 2023: 8958962, 2023.
31. Zhang L, Li Y, Dai Y, Wang D, Wang X, Cao Y, Liu W and Tao Z: Glycolysis-related gene expression profiling serves as a novel prognosis risk predictor for human hepatocellular carcinoma. Sci Rep 11: 18875, 2021.
32. Shao F, Ling L, Li C, Huang X, Ye Y, Zhang M, Huang K, Pan J, Chen J and Wang Y: Establishing a metastasis-related diagnosis and prognosis model for lung adenocarcinoma through CRISPR library and TCGA database. J Cancer Res Clin Oncol 149: 885-899, 2023.
33. Zhu Y, Sun L, Yu J, Xiang Y, Shen M, Wasan HS, Ruan S and Qiu S: Identification of biomarkers in colon cancer based on bioinformatic analysis. Transl Cancer Res 9: 4879-4895, 2020.
34. Shen X and Han J: Overexpression of gene DEP domain containing 1 and its clinical prognostic significance in colorectal cancer. J Clin Lab Anal 34: e23634, 2020.
35. Kim J: In silico analysis of differentially expressed genesets in metastatic breast cancer identifies potential prognostic biomarkers. World J Surg Oncol 19: 188, 2021.
36. Yang M, Zhang H, Gao S and Huang W: DEPDC1 and KIF4A synergistically inhibit the malignant biological behavior of osteosarcoma cells through Hippo signaling pathway. J Orthop Surg Res 18: 145, 2023.
37. Jia B, Liu J, Hu X, Xia L and Han Y: Pan-cancer analysis of DEPDC1 as a candidate prognostic biomarker and associated with immune infiltration. Ann Transl Med 10: 1355, 2022.
38. Harada Y, Kanehira M, Fujisawa Y, Takata R, Shuin T, Miki T, Fujioka T, Nakamura Y and Katagiri T: Cell-permeable peptide DEPDC1-ZNF224 interferes with transcriptional repression and oncogenicity in bladder cancer cells. Cancer Res 70: 5829-5839, 2010.
39. Zhou C, Wang P, Tu M, Huang Y, Xiong F and Wu Y: DEPDC1 promotes cell proliferation and suppresses sensitivity to chemotherapy in human hepatocellular carcinoma. Biosci Rep 39: BSR20190946, 2019.
40. Feng X, Zhang C, Zhu L, Zhang L, Li H, He L, Mi Y, Wang Y, Zhu J and Bu Y: DEPDC1 is required for cell cycle progression and motility in nasopharyngeal carcinoma. Oncotarget 8: 63605-63619, 2017.
41. Obara W, Ohsawa R, Kanehira M, Takata R, Tsunoda T, Yoshida K, Takeda K, Katagiri T, Nakamura Y and Fujioka T: Cancer peptide vaccine therapy developed from oncoantigens identified through genome-wide expression profile analysis for bladder cancer. Jpn J Clin Oncol 42: 591-600, 2012.
42. Guo W, Li H, Liu H, Ma X, Yang S and Wang Z: DEPDC1 drives hepatocellular carcinoma cell proliferation, invasion and angiogenesis by regulating the CCL20/CCR6 signaling pathway. Oncol Rep 42: 1075-1089, 2019.
43. Alorjani M, Aburub M, Al-Trad B, Hamad MA, AbuAlarja M, Bashir SA, Al-Batayneh K and Zoubi MA: The prevalence of CHEK1 and CHEK2 mutations in prostate cancer: A retrospective cohort Study. Med Arch 77: 8-12, 2023.
44. Chen Y, Zhang S, Li Z, Yin B, Liu Y and Zhang L: Discovery of a dual-target inhibitor of CDK7 and HDAC1 that induces apoptosis and inhibits migration in colorectal cancer. ChemMedChem 18: e202300281, 2023.
45. Landsburg DJ, Morrissette JJ, Nasta SD, Barta SK, Schuster SJ, Svoboda J, Chong EA and Bagg A: TP53 mutations predict for poor outcomes in patients with newly diagnosed aggressive B-cell lymphomas in the current era. Blood Adv 7: 7243-7253, 2023.